Design and Optimization of an Axial Expansion Turbine for Energy Recovery

Octavian-Valentin Nemet
Hydrodynamics and Hydraulic Machines
Politehnica University Timişoara, România
octavian@nemet.ro

Adrian Ciprian Stuparu
Hydrodynamics and Hydraulic Machines
Politehnica University Timişoara, România
adrian.stuparu@upt.ro

Romeo Florin Susan-Resiga
Hydrodynamics and Hydraulic Machines
Politehnica University Timişoara, România
romeo.resiga@upt.ro

***Abstract* - The paper presents a methodology for designing the stator and rotor blades for an axial expansion turbine, with optimisation procedure with respect to cavitation behaviour. The resulting stator-rotor thin blades tandem is analysed using unsteady, incompressible and inviscid flow simulation in order to validate the quasi-analytical design method and associated computer code. Finally, thickness is added to the thin blade (camberline) to insure structural integrity and the resulting configuration is analyzed in turbulent flow.**

***Index Terms* - Hydraulic turbines, Design optimization.**

I. Introduction

Fluids from many industrial processes are often released via pressure regulators or valves thus dissipating (wasting) their hydraulic energy excess. The overall efficiency of the process can be improved by recovering the hydraulic energy, as mechanical then electrical energy, through modular axial-expansion turbines (AXENT) which were developed in the last decades [1]. Their main advantage over other turbines is that they do not generate a significant pressure surge in the event of a power failure or blocking the machine, having thus no negative impact on the process by their installation.

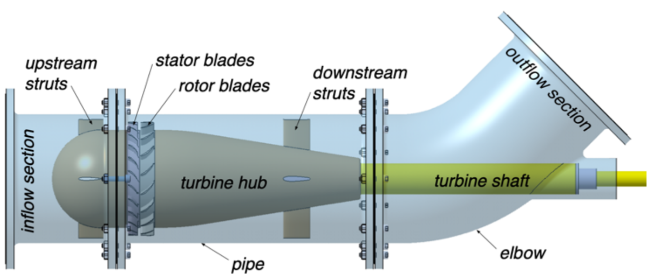

Figure 1. Typical axial expansion turbine for energy recovery.

Fig. 1 shows a sketch of an axial expansion turbine for energy recovery. The incoming pipe flow is accelerated in the annular space between the hub and the pipe, where the stator and rotor blade rows are located. Further downstream the flow is decelerated practically back to the upstream discharge velocity, and the elbow allows the shaft to be connected to the electrical generator. The goal of this paper is to present a methodology for designing and optimizing the blades.

The design example presented in this paper starts with the main parameters of the turbine as follows [1,2]:

- Pipe diameter $D_p = 220\,mm$,
- Volumetric discharge $Q = 0.07\,m^3/s$,
- Turbine head $H = 24\,m$,
- Runner speed $n = 1500\,rpm$.

Using these main parameters, one can compute the hub diameter, as we have shown in [2]. Essentially, using the theory of pipe swirling flow with stagnant region, the hub diameter is chosen such as to fill completely the predicted stagnant region. In our case, it results a hub diameter $D_h = 188\,mm$. The average axial velocity in the annular space between the hub and the pipe, corresponding to the design volumetric discharge, results as $V_a = 6.8\,m/s$.

The main focus of the paper is to present a methodology for optimal blade design. The present methodology uses a quasi-analytical approach for blade design, with a specific parameterization of the blade loading distribution. Other optimization approaches [3] use a full 3D CFD simulation coupled with genetic algorithms. In doing so, we consider hydrofoil cascades for both the stator and the rotor of the turbine, at an average (from discharge point of view) radius between hub and shroud $R = \sqrt{\left(R_p^2 + R_h^2\right)/2} = 0.102\,m$. The tangential transport velocity at this radius, corresponding to the runner speed above, is $U = 16.0\,m/s$.

The paper is organized as follows. Section II presents the quasi-analytical thin hydrofoil cascade design, and the parameterization used for the optimization. The quasi-analytical results, and the associated design computer code, are validated by direct numerical simulation of the inviscid, incompressible, unsteady flow in the two blade rows. Section III presents an approach for adding blade thickness in order to insure structural integrity and presents a turbulent flow simulation. The paper conclusions are summarized in the last section.

II. THIN HYDROFOIL CASCADE DESIGN

A. The cascade design problem

A cascade of hydrofoils is a periodic arrangements of identical hydrofoils (blades) with the spacing (pitch) s, considered here in dimensionless form by scaling it with the cascade axial width. For an axial turbomachine, the cascade is a simplified model generated by cutting the blades with a cylindrical surface at a radius between hub and shroud. The axial direction, given by the unit vector $\hat{\boldsymbol{e}}_a$, is normal to the cascade straight front line (connecting the hydrofoils leading edges), and the tangential direction $\hat{\boldsymbol{e}}_u$ is along the front line. Let us denote the upstream uniform flow by ① and the downstream one by ②. Upstream the cascade the axial velocity component is $V_{a\textcircled{1}}$, the tangential component $V_{u\textcircled{1}}$, and the corresponding flow direction is $\tan\alpha_{\textcircled{1}} = V_{u\textcircled{1}} / V_{a\textcircled{1}}$ where $\alpha_{\textcircled{1}}$ is the flow angle with respect to the axial direction. Downstream the cascade the uniform flow direction is $\tan\alpha_{\textcircled{2}} = V_{u\textcircled{2}} / V_{a\textcircled{2}}$. Thanks to the continuity equation the axial velocity component upstream and downstream the cascade is the same, $V_{a\textcircled{1}} = V_{a\textcircled{2}} = V_a$.

The cascade design problem essentially asks for the hydrofoil shape with given upstream/downstream flow directions, $\tan\alpha_{\textcircled{1}}$ and $\tan\alpha_{\textcircled{2}}$, respectively, and given pitch s. Within this framework, the hydrofoil shape as well as the pressure distribution on the foil are determined by assuming a pitch-average vorticity dV_u / dx variation from the leading edge, $x = 0$ up to the trailing edge $x = 1$. If $f_0(x), x \in [0,1]$ denotes the generic streamline for the pitch-average flow that turns in the bladed region, then $f_0'(x)$ is the flow direction and $f_0''(x)$ is the corresponding vorticity,

$$\begin{aligned}
f_0''(x) &= \left(\tan\alpha_{\textcircled{2}} - \tan\alpha_{\textcircled{1}}\right) g(x) \\
f_0'(x) &= \tan\alpha_{\textcircled{1}} + \left(\tan\alpha_{\textcircled{2}} - \tan\alpha_{\textcircled{1}}\right) \int_0^x g(t)\,dt, \\
f_0(x) &= x\tan\alpha_{\textcircled{1}} + \left(\tan\alpha_{\textcircled{2}} - \tan\alpha_{\textcircled{1}}\right) \int_0^x \left(\int_0^s g(t)\,dt \right) ds.
\end{aligned} \tag{1}$$

The function $g(x)$ describes the blade loading distribution. Since $f_0'(0) = \tan\alpha_{\textcircled{1}}$ and $f_0'(1) = \tan\alpha_{\textcircled{2}}$, the integral of $g(x)$ from 0 to 1 should be equal to 1. In addition, thanks to the Kutta-Joukowski condition at the trailing edge, it is mandatory that $g(1) = 0$. An unloaded leading edge would also require $g(0) = 0$, but this is a design option.

The above approach is called *inverse design method* since one prescribes (optimizes) the flow then the blade shape follows. The classical *direct design method* optimizes the parameterized blade geometry by choosing various objective functions. In our case, we choose a parametric blade loading distribution, $g(x;\lambda_1,\lambda_2,\ldots)$ and determine the parameters λ_i by minimizing the maximum velocity on the blade, thus insuring the best cavitational behavior.

Once the pitch-average flow described according to Eqs. (1) one can iteratively compute the thin blade shape $f(x)$ (i.e. the camberline) from the integro-differential equations [4]

$$\begin{aligned}
f(x) &= \frac{x}{2}\left(\tan\alpha_{\textcircled{1}} + \tan\alpha_{\textcircled{2}}\right) + \int_0^1 F_2(x,t)\,dt \\
&+ \frac{s}{2\pi}\left(\tan\alpha_{\textcircled{2}} - \tan\alpha_{\textcircled{1}}\right) g(x) \times \\
&\left[\begin{array}{l} \ln\left(2\pi/s\right) + \dfrac{1}{2}\ln\left(\dfrac{1+f'^2(x)}{2}\right) \\ + x\ln x + (1-x)\ln(1-x) - 1 \end{array}\right], \text{ where} \\
F_2(x,t) &= \frac{s}{4\pi}\left(\tan\alpha_{\textcircled{2}} - \tan\alpha_{\textcircled{1}}\right) \times \\
&\left\{\begin{array}{l} g(t)\ln\left[\dfrac{\cosh\frac{2\pi}{s}(x-t) - \cos\frac{2\pi}{s}\left(f(x)-f(t)\right)}{\cosh\frac{2\pi}{s}t - \cos\frac{2\pi}{s}f(t)}\right] \\ - g(x)\ln\left[\left(\dfrac{2\pi}{s}(x-t)\right)^2 \dfrac{1+f'^2(x)}{2}\right] \end{array}\right\}
\end{aligned} \tag{2}$$

$$\begin{aligned}
\frac{df}{dx}(x) &= \frac{\tan\alpha_{\textcircled{1}} + \tan\alpha_{\textcircled{2}}}{2} + \int_0^1 F_1(x,t)\,dt \\
&+ \frac{s}{2\pi}\left(\tan\alpha_{\textcircled{2}} - \tan\alpha_{\textcircled{1}}\right) g(x)\ln\frac{x}{1-x}, \text{ where} \\
F_1(x,t) &= \left(\tan\alpha_{\textcircled{2}} - \tan\alpha_{\textcircled{1}}\right) \times \\
&\left\{\begin{array}{l} \dfrac{g(t)}{2}\dfrac{\sinh\frac{2\pi}{s}(x-t) + f'(x)\sin\frac{2\pi}{s}\left(f(x)-f(t)\right)}{\cosh\frac{2\pi}{s}(x-t) - \cos\frac{2\pi}{s}\left(f(x)-f(t)\right)} \\ - \dfrac{s}{2\pi}g(x)\dfrac{1}{x-t} \end{array}\right\}
\end{aligned} \tag{3}$$

Basically, for the first iteration one inserts in the right-hand side of Eqs. (2) and (3) the functions $f_0(x)$ and $f_0'(x)$ from Eqs. (1). Then, the updated functions from the left-hand side are used to evaluate the right-hand expressions. This iterative process is repeated until $f(x)$ practically does not change anymore [5].

Once the thin blade shape (camberline) $f(x)$ computed, one can evaluate the velocity on both sides of the foil. First, the average blade velocity $V_{bl}(x)$ is computed as

$$\frac{V_{bl}(x)}{V_a} = \frac{1+f'(x)f_0'(x)}{\sqrt{1+f'^2(x)}} + \frac{\tan\alpha_{②} - \tan\alpha_{①}}{2\sqrt{1+f'^2(x)}} \times \int_0^1 \left[\frac{f'(x)\sinh\frac{2\pi}{s}(x-t) - \sin\frac{2\pi}{s}\left(f(x)-f(t)\right)}{\cosh\frac{2\pi}{s}(x-t) - \cos\frac{2\pi}{s}\left(f(x)-f(t)\right)} - f'(x)\,\mathrm{sgn}(x-t) \right] g(t)\,dt, \tag{4}$$

then the velocities on both sides are evaluated as

$$\frac{V_{bl}^{\pm}(x)}{V_a} = \frac{V_{bl}(x)}{V_a} \pm \frac{1}{2}\frac{\left(\tan\alpha_{②} - \tan\alpha_{①}\right) s\, g(x)}{\sqrt{1+f'^2(x)}}. \tag{5}$$

The pressure follows from the Bernoulli theorem.

The above algorithm is implemented by discretizing $f(x)$ with piecewise cubic polynomials [5,6] using the PCHIP (Piecewise Cubic Hermite Interpolation Package) available in the SLATEC Common Mathematical Library [7]. The integrals are evaluated by numerical quadrature using the QUADPACK subroutines also available in the SLATEC library.

B. Design and optimization of thin blades stator-rotor cascades

In order to design the cascades for both stator and rotor blades we first choose a parameterization of the loading function as

$$g(x;\lambda_1,\lambda_2,\lambda_3) = \mathrm{erf}\left(\lambda_1 x\right) \times \mathrm{erf}\left(\lambda_2(1-x)\right) \times \left(1+\lambda_3 x\right). \tag{6}$$

The loading function is scaled by its integral from 0 to 1. A two-parameter loading function has been successfully employed in [8] for a pump inducer optimization.

One can see that the expression (6) vanishes both at the leading edge, $x=0$ and trailing edge $x=1$. The parameters control the slope of the loading distribution at leading edge, trailing edge and in the middle, respectively. The objective function to be minimized is the maximum velocity on the blade, as computed with (5).

According to the design operating point, for the stator cascade we have $\tan\alpha_{①}=0$, and $\tan\alpha_{②} = V_{u②}/V_a$. For the rotor cascade we compute the relative flow, thus we have $\tan\beta_{②} = \left(V_{u②} - U\right)/V_a$ at the stator-rotor interface and $\tan\beta_{③} = -U/V_a$ downstream the rotor, denoted by ③. Both cascades have the same pitch $s=1$, consistent with the Zweifel criterion [9].

The optimization procedure for the thin blade design uses the *maximum velocity on the blade as the objective function to be minimized* by automatically adjusting the three parameters in (6) with the BOBYQA algorithm for bound constrained optimization without derivatives [10].

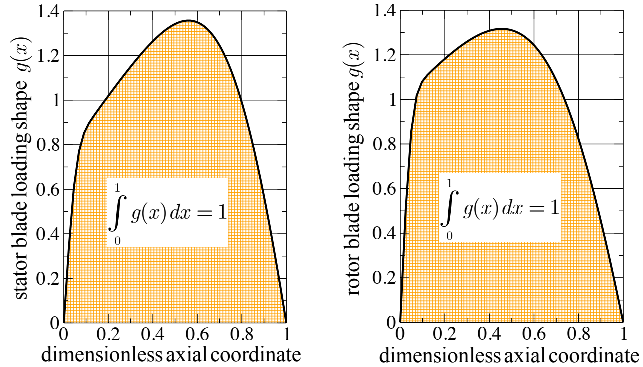

Figure 2. Stator (left) and rotor (right) optimum blade loading shape.

The resulting blade loading distributions for both stator and rotor blades are shown in Fig. 2.

The design in-house code developed by the authors is validated by a numerical simulation of the tandem stator-rotor cascade flow using the FLUENT expert code. The 2D unsteady, incompressible and inviscid flow is solved simultaneously for the stator and rotor periodic domains, Fig. 3, using the sliding mesh technique. While the stator domain is fixed, the rotor is moving with the transport velocity U. The velocity triangles at the stator-rotor interface and rotor outlet, respectively, are shown in Fig. 3. Note that the flow upstream the stator, as well as downstream the rotor, is axial at the design operating point. At off design regimes there will be a residual swirl downstream the rotor. The streamlines for the absolute stator flow and relative rotor flow, respectively, Fig. 3, show the shock-free flow at the leading edge of the blades.

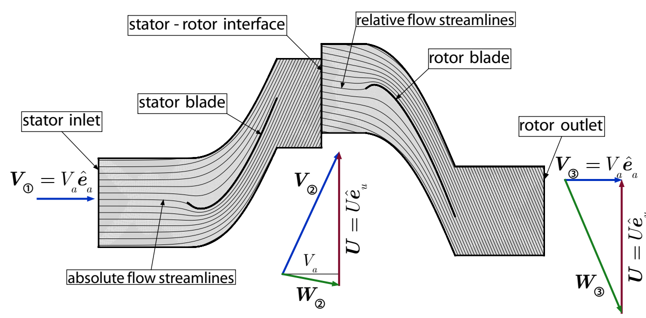

Figure 3. Flow kinematics of stator-rotor tandem cascades. Streamlines for the absolute stator flow and for the relative rotor flow. Velocity triangles upstream and downstream the rotor cascade.

$$\begin{aligned} c_p &\equiv \frac{p - p_{③}}{\rho V_a^2/2} && \text{definition} \\ &= 1 + 2\frac{V_{u②}}{V_a}\frac{U}{V_a} - \left(\frac{V}{V_a}\right)^2 && \text{stator absolute flow} \\ &= 1 + \left(\frac{U}{V_a}\right)^2 - \left(\frac{W}{V_a}\right)^2 && \text{rotor relative flow} \end{aligned} \tag{7}$$

The actual validation of the design code, is done by comparing the pressure coefficient on the blades obtained from the theoretical velocity distribution (5), with the appropriate Bernoulli theorems for absolute and relative flows, with the directly computed values in FLUENT using the pressure values on the blades, as shown in Eqs (7). Fig. 4 shows the pressure coefficient directly computed from the FLUENT numerical simulation, solid lines, and the values from the quasi-analytical theory employed in the design process, circles. Obviously, the agreement is excellent within the numerical errors margin.

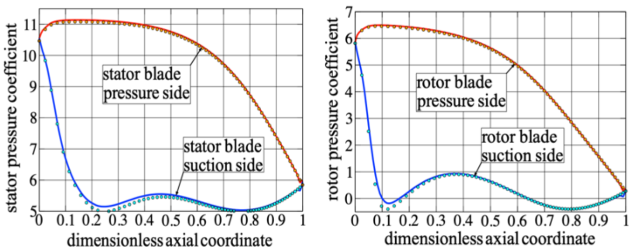

Figure 4. Stator (left) and rotor (right) pressure coefficient. The circles correspond to the theoretical values computed from the design code and the solid lines are from the FLUENT numerical solution.

Using the expression for the pressure coefficient in the stator one can immediately obtain the overall pressure drop as $p_{\textcircled{1}} - p_{\textcircled{3}} = \rho U V_{u\textcircled{2}}$, which is the same as the total pressure drop in our case for the design operating point with plain axial flow both upstream the stator and downstream the rotor.

III. Thick Blade Cascades in Real Flow

The thin blade design methodology provides the camberline of the blade. For real blades thickness must be added to the camberline to insure structural integrity. For the present paper we have adopted the YS-900 symmetric hydrofoil [11] thickness distribution for the blade thickness in the tangential direction. The thickness function is scaled-up for a maximum of 10% blade blockage at 52.5% axial width from the leading edge. The corresponding thick stator and rotor blades are shown in Fig. 5. A direct thick blade optimization using the similar approach employed in this paper has been attempted in [12].

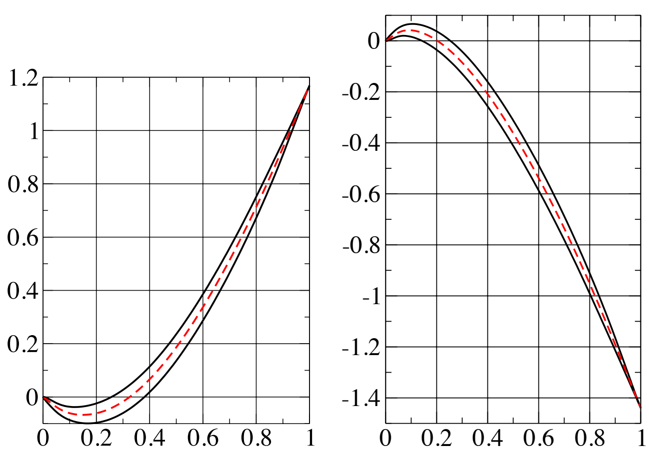

Figure 5. Stator (left) and rotor (right) thick blades.

We emphasize once more that the blade thickness, traditionally considered in the direction locally normal to the camberline, is obtained by enforcing the chosen tangential thickness, borrowed from a symmetric hydrofoil.

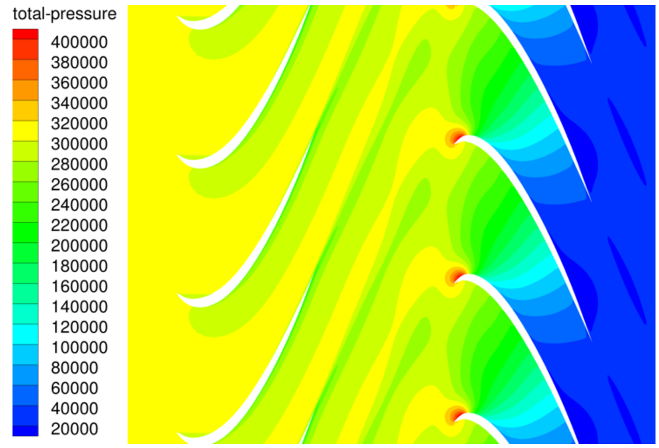

Figure 6. Total pressure in the stator and rotor blade cascades.

Finally, the thick blades rotor-stator cascades are assessed in viscous flow simulation, using in our case the Spalart and Allmaras turbulence model [13]. Fig. 6 shows the total pressure map obtained in this case, as an illustration of the specific hydraulic energy evolution in the bladed region. Upstream the rotor blades the total pressure practically remains constant except the boundary layers and subsequent wakes of the stator blades. Within the rotor blades row the total pressure decreases corresponding to the conversion of hydraulic energy in mechanical energy. Also, the total pressure has an increase at the leading edge (red spots) as usual in turbine cascades.

IV. Conclusions

The paper presents a complete methodology for robust and optimum design of the blades for an axial expansion turbine. The core design algorithm employs a quasi-analytical approach for the thin blade cascades, with an optimization with respect to the cavitation behavior. Practically, the objective function to be minimized in the optimization process corresponds to the maximum velocity on the blades. Then, a thickness distribution is added to the camberline to insure structural integrity. Since the design procedure assumes an inviscid incompressible flow, a viscous flow simulation completes the performance evaluation of the design. The present methodology practically eliminates the classical trial-and-error direct approach, providing an optimized configuration customized to the specific process served by the energy recovery turbine.

References

[1] A. Neipp, "Ein- und zweistufige axiale Entspannungsturbine zur Energiegewinnung," PhD. Dissertation, Institut für Strömungsmechanik und Hydraulische Strömungsmaschinen, Universtät Stuttgart, 2017.

[2] R. F. Susan-Resiga, S. Muntean, A. Stuparu, A. Neipp, A. Ruprecht, and S. Riedelbauch, "On the Hub-to-Shroud Ratio of an Axial Expansion Turbine for Energy Recovery," in *Proc. 6th IAHR Int. Meeting of the Workgroup on Cavitation and Dynamic Problems in Hydraulic Machinery and Systems*, Sep. 9-11, Ljubljana, Slovenia, 2015. http://iahrwg2015.si/files/papers/2_Analysis_of_pumps_turbines_and_pump_turbines/ON_THE_HUB_TO_SHROUD_RATIO_OF_AN_AXIAL_EXPANSION_TURBINE_FOR_ENERGY_RECOVERY.pdf

[3] A. Neipp and S. Riedelbauch, "Automated CFD flow optimization of an Axial Expansion Turbine for Energy Recovery from Working Fluids," n *Proc. 6th IAHR Int. Meeting of the Workgroup on Cavitation and Dynamic Problems in Hydraulic Machinery and Systems*, Sep. 9-11, Ljubljana, Slovenia, 2015.

http://iahrwg2015.si/files/papers/2_Analysis_of_pumps_turbines_and_pump_turbines/IAHR_WG_15_2_4_Neipp.pdf

[4] W. R. Hawthorne, C. Wang, C. S. Tan, and J. E. McCune, “Theory of Blade Design for Large Deflections: Part I – Two Dimensional Cascade,” *Journal of Engineering for Gas Turbines and Power – Transactions of the ASME*, vol. 106, pp. 346-353, Apr. 1984.

[5] R. F. Susan-Resiga, S. Muntean, S. Bernad, T. Frunză, and D. Balint, „Thin Hydrofoil Cascade Design and Numerical Flow Analysis. Part I - Design,” *Proc. of the Romanian Academy, Series A*, vol. 7(2), pp. 117-126, 2006. https://academiaromana.ro/sectii2002/proceedings/doc2006-2/05-Resiga-1.pdf

[6] R. F. Susan-Resiga, S. Muntean, S. Bernad, T. Frunză, and D. Balint, „Thin Hydrofoil Cascade Design and Numerical Flow Analysis. Part II - Analysis,” *Proc. of the Romanian Academy, Series A*, vol. 7(3), 2006. https://academiaromana.ro/sectii2002/proceedings/doc2006-3/05-Resiga-2.pdf

[7] F. N. Fritsch, “Piecewise Cubic Hermite Interpolation Package,” Lawrence Livermore National Laboratory, Rep. UCRL-87285, Jul. 1982.

[8] I. G. Moisă, R. F. Susan-Resiga, and S. Muntean, „Pump Inducer Optimization Based on Cavitation Criterion,” *Proc. of the Romanian Academy, Series A*, vol. 14(4), pp. 317-325, 2013. https://academiaromana.ro/sectii2002/proceedings/doc2013-4/08-Resiga.pdf

[9] S. L. Dixon and C. A. Hall, *Fluid Mechanics and Thermodynamics of Turbomachinery*, 7th ed., Elsevier, 2014, p. 102.

[10] M. J. D. Powell, “The BOBYQA algorithm for bound constrained optimization without derivatives,” Dpt. Applied Mathematics and Theoretical Physics, University of Cambridge, Rep. DAMPT NA06, 2009,http://www.damtp.cam.ac.uk/user/na/NA_papers/NA2009_06.pdf

[11] R. Eppler and Y. T. Shen, „Wing Sections for Hydrofoils – Part 1: Symmetrical Profiles,” Journal of Ship Research, vol. 23(3), pp. 209-217, 1979.

[12] T. Frunză, R. F. Susan-Resiga, S. Muntean, and S. Bernad, „Optimization of the hydrofoil cascade and validation with quasi-analytical solution for hydraulic machinery,” in *Proc. 25th IAHR Symposium on Hydraulic Machinery and Systems*, IOP Conf. Series: Earth and Environmental Science, vol 12, p. 012075, 2010. https://iopscience.iop.org/article/10.1088/1755-1315/12/1/012075/pdf

[13] P. Spalart and S. Allmaras, „A one-equation turbulence model for aerodynamics flows,” Americal Institute of Aeronautics and Astronautics, Technical Report AIAA-92-0439, 1992.